

Theoretical Simulations of the Structural Stability, Elastic, Electronic, Magnetic and Thermodynamic Properties of New Half-metallic $\text{Cr}_2\text{GdSn}_{1-x}\text{Pb}_x$ Alloys

I. Asfour*

Département de Technologie des Matériaux, Faculté de Physique, Université des Sciences et de la Technologie d'Oran Mohamed Boudiaf (USTO-MB), BP 1505, El M'naouer, 31000 Oran, Algeria

(Received 21 June 2021; revised manuscript received 15 August 2021; published online 25 August 2021)

Based on full-potential linearized augmented plane wave (FP-LAPW) method within the density functional theory (DFT), the structural, elastic, electronic, magnetic, thermodynamic and thermal properties of quaternary Heusler $\text{Cr}_2\text{GdSn}_{1-x}\text{Pb}_x$ alloys have been studied under the generalized gradient approximation (GGA). The structural properties show the stability of $\text{Cr}_2\text{GdSn}_{1-x}\text{Pb}_x$ alloys in the ferromagnetic phase, where their equilibrium structural parameters (lattice constant $a(\text{Å})$, bulk modulus $B(\text{GPa})$ and its first-pressure derivative (B') are evaluated. The elastic constants for the cubic system (C_{11} , C_{12} , and C_{44}) and anisotropy are computed to prove the mechanical stability of these compounds. The electronic results reveal that both $\text{Cr}_2\text{GdSn}_{1-x}\text{Pb}_x$ alloys have a perfect half-metallic nature. The magnetic properties reveal that the total magnetic moment of cubic Cr_2GdSn and Cr_2GdPb compounds is equal to $-12\mu_B$ and $-11\mu_B$, respectively, affirming their complete half-metallic behavior. The quasi-harmonic Debye model, as implemented in the Gibbs code, was used to predict the thermal properties of $\text{Cr}_2\text{GdSn}_{1-x}\text{Pb}_x$. These alloys seem to be a potential candidate of spintronic devices.

Keywords: FP-LAPW, Electronic properties, Ferromagnetic, Half-metallic, Debye model.

DOI: [10.21272/jnep.13\(4\).04017](https://doi.org/10.21272/jnep.13(4).04017)

PACS numbers: 63.70. + h, 75.50.Cc

1. INTRODUCTION

In 1903, the history of Heusler materials began. Fritz Heusler discovered that the formula Cu_2MnAl behaves like a ferromagnetic material, knowing that its components are not the same magnetic materials [1], that attracted exceptional attention of many scientists to the study and understanding of their potential properties, thermal and thermoelectric characteristics [2]. The Heusler alloys have attracted a great deal of attention being among the most important material systems used in many fields: optoelectronic [3], superconductivity, shape memory and thermoelectric [4]. The Heusler ternary alloys are determined by the generic formulas X_2YZ or XYZ [5, 6]. In X_2YZ Heusler alloys, X and Y are transition metals and Z is an element of group III, IV or V, in some cases, Y is replaced by a rare earth element. The X_2YZ Heusler compounds crystallize in the cubic L_{21} (AlCu_2Mn -type) structure with the space group $\text{Fm}\bar{3}\text{m}$. The X, Y and Z atoms in this structure are located on the Wyckoff positions $8c$ ($1/4, 1/4, 1/4$), $4a$ ($0, 0, 0$) and $4b$ ($1/2, 1/2, 1/2$), respectively. The cubic X_2YZ compounds can also be found in the CuHg_2Ti type structure with the space group $\text{F}\bar{4}3\text{m}$. Contrary to the L_{21} structure, two X atoms occupy nonequivalent positions for this structure.

This structure is frequently observed when the nuclear charge of the Y element is larger than that of the X element of the same period, that is $Z(\text{Y}) > Z(\text{X})$ for two $3d$ transition metals. The X atoms are located on Wyckoff positions $4a$ ($0, 0, 0$) and $4c$ ($1/4, 1/4, 1/4$), while Y and Z atoms are located, respectively, on $4b$ ($1/2, 1/2, 1/2$) and $4d$ ($3/4, 3/4, 3/4$) positions [7]. Recently, we calculated the electronic and magnetic properties of Heusler Cr_2GdSn alloys using the ab-initio method in

the GGA scheme [8]. In this paper, we focused our study on the structural, electronic, magnetic and thermal properties of $\text{Cr}_2\text{GdSn}_{1-x}\text{Pb}_x$ ($x = 0, 0.25, 0.50, 0.75, 1.00$) compounds. The rest of the paper is arranged as follows: section 2 includes computational details and the method of calculation, section 3 is devoted to the results and discussion, and section 4 is a summary of our conclusions.

2. COMPUTATIONAL METHODS

In this report, the calculations were done using density functional theory (DFT) [9] within the framework of the full-potential linearized augmented plane-wave (FP-LAPW) method as implemented in WIEN2K package [10]. The generalized-gradient approximation (GGA) was used for the exchange correlation potential [11]. We chose the muffin-tin (MT) radii for the Cr, Gd, Sn and Pb atoms to be 2.1, 2.3, 1.7 and 2.1 Bohr, respectively. The plane wave cut-off parameter was taken as $\text{RMT}^*K_{\text{max}} = 9$, the Monkhorst-Pack special k -points were performed using 3000 special k -points in the Brillouin zone [15]. The power-cut zone, which defines the separation of the valence and core states, was chosen as -6.0 Ry. In order to simulate $\text{Cr}_2\text{GdSn}_{1-x}\text{Pb}_x$ ($x = 0.25, 0.50, 0.75$) quaternary alloy, we created a supercell with 16 atoms. For $x = 0.25$, we substituted one atom of Sn by one atom of Pb; for $x = 0.50$, we substituted two atoms of Sn by two atoms of Pb; for $x = 0.75$, we substituted three atoms of Sn by three atoms of Pb. The study of thermal effects was done within the quasi-harmonic Debye model implemented in the Gibbs program [8]. The quasi-harmonic Debye model allows us to obtain all thermodynamics quantities from the calculated energy-volume points. Detailed description of this procedure can be found in Refs. [8, 12].

* asfissam@gmail.com
issam.asfour@univ-usto.dz

3. RESULTS AND DISCUSSION

3.1 Structural Properties

We calculated the lattice constant (a), the bulk modulus (B), and its first derivative (B') by optimization of the total energy (E_T) versus volume (V) using the Murnaghan equation of state [14]. We focused on the structural properties of $\text{Cr}_2\text{GdSn}_{1-x}\text{Sb}_x$ quaternary Heusler alloys such as the lattice parameter and bulk modulus. To obtain the equilibrium lattice constant and determine the stable structure of these alloys, we performed structural optimization of Cr_2GdSb alloy for nonmagnetic (NM) and ferromagnetic (FM) configurations in their two possible structures: $L2_1$ and X-type. It is clearly seen that these structures are more stable in the $L2_1$ than in the X-type (Fig. 1). For Cr_2GdPb in the $L2_1$ structure, our work yields a lattice constant of 6.5997 Å.

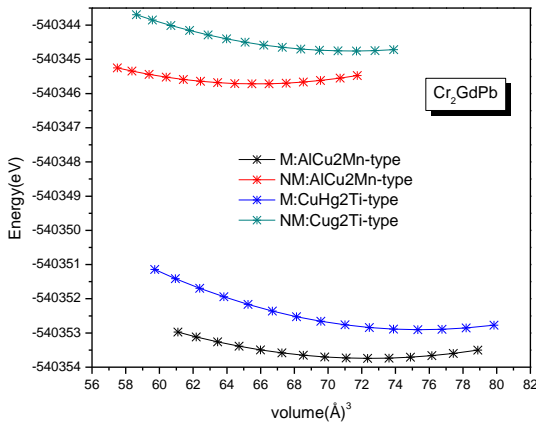


Fig. 1 – Total energy of Cr_2GdSb compound as a function of volume for nonmagnetic (NM) and magnetic (M) states of AlCu_2Mn and CuHg_2Ti structures

The second step of our calculations was to study the structural properties of $\text{Cr}_2\text{GdSn}_{1-x}\text{Pb}_x$ quaternary Heusler alloys, we used a supercell model compatible with the percentage of constituents in question. The lattice structures were modeled at some selected compositions $x = 0.25, 0.5$ and 0.75 . For the considered structures, the lattice parameters and bulk modulus as a function of composition x are listed in Table 1. For $\text{Cr}_2\text{GdSn}_{0.75}\text{Pb}_{0.25}$, $\text{Cr}_2\text{GdSn}_{0.50}\text{Pb}_{0.50}$ and $\text{Cr}_2\text{GdSn}_{0.25}\text{Pb}_{0.75}$ in the Cu_2MnAl -type structure, the lattice constant obtained in this work is 6.6596 Å, 6.6364 Å and 6.6183 Å, respectively. We want to make it clear that there are no results on the lattice constant so far in the literature or experiments, our results are considered as purely predictive. It was found that they vary almost linearly following the Vegard's law [15]. A slight deviation from the Vegard's law is clearly visible for the alloy with a bowing upwardly parameter equal to 0.0291 Å. The bulk modulus increases slightly on going from Cr_2GdSn to Cr_2GdSb showing a non-linear behavior.

Fig. 2 shows the variation of the lattice parameter calculated based on the concentration of tin for the quaternary alloy. A slight deviation from the Vegard's law is clearly visible for the alloy with a bowing upwardly parameter equal to 0.0291 Å obtained by adjusting the values calculated by a polynomial function. The

physical origin of this small gap could be mainly due to the small mismatch between the lattice constants of Cr_2GdSn and Cr_2GdPb ternary compound. Fig. 3 represents the variation of the bulk modulus as a function of the antimony concentration in $\text{Cr}_2\text{GdSn}_{1-x}\text{Sb}_x$ alloys. The disorder parameter equal to -4.1081 GPa for $\text{Cr}_2\text{GdSn}_{1-x}\text{Pb}_x$ alloys shows that the bulk modulus increases with increasing Pb concentration ($0 \leq x \leq 1$).

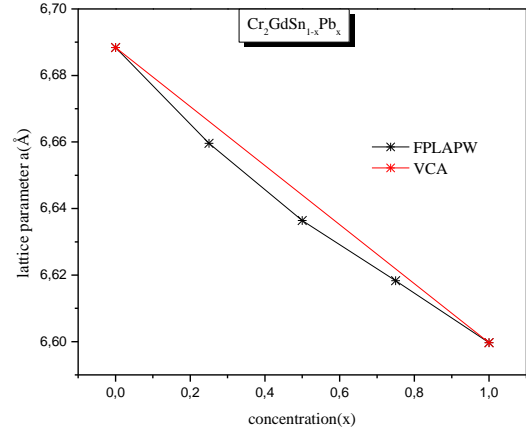


Fig. 2 – The lattice parameters of $\text{Cr}_2\text{GdSn}_{1-x}\text{Pb}_x$ as a function of Pb composition

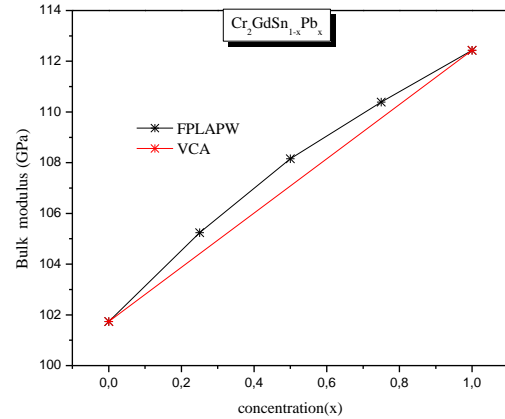


Fig. 3 – Variation of the bulk modulus of $\text{Cr}_2\text{GdSn}_{1-x}\text{Pb}_x$ Heusler alloys with Pb concentration x

3.2 Mechanical and Elastic Properties

As stated above, the purpose of our work is also to examine the variation in the elastic and mechanical properties of our compounds. In particular, we will confirm their mechanical stability via calculation of the elastic constants C_{ij} . These constants are fundamental and indispensable for describing the mechanical properties of materials that undergo stress and give important information concerning the binding characteristic between adjacent atomic planes, mechanical stability and anisotropic character of binding.

The symmetry of the cubic crystal reduces the number of constants C_{ij} to only three independent elastic constants C_{11} , C_{12} and C_{44} . Further details of the calculation can be found elsewhere [14]. The following mechanical quantities: the calculated three independent elastic constants C_{11} , C_{12} and C_{44} , shear modulus G , B/G ratio, Young's modulus E , Poisson's ratio (ν), Zener

anisotropy factor (A) and density (ρ) of $\text{Cr}_2\text{GdSn}_{1-x}\text{Pb}_x$ for various compositions are listed in Table 1 using the standard relations reported elsewhere [15]. We did not find results for elastic constants that are available in the literature. Therefore, our results are considered as purely predictive. The mechanical stability criteria for cubic crystals at equilibrium are expressed by elastic constants as follows: $C_{11} - C_{12} > 0$, $C_{44} > 0$, $C_{11} + 2C_{12} > 0$ and $C_{12} < B < C_{11}$ [17]. We notice that the calculated elastic constants satisfy the above stability criteria. We can say that these compounds are elastically stable. Fig. 4 represents the variation of the elastic constants as a function of the composition x . We observe that the elastic constants C_{11} , C_{44} increase monotonically with x , indicating that on going from $x=0$ (Cr_2GdSn) to $x=1$ (Cr_2GdSb) the alloy structure becomes mechanically stable.

The following equations show the value of the disorder:

$$C_{11} = 252.0939 - 32.4993x + 4.3496x^2,$$

$$C_{12} = 156.3294 - 27.3553x + 7.3749x^2,$$

$$C_{44} = 50.2046 - 8.9974x + 2.5462x^2.$$

The values of the disorder for C_{11} , C_{12} and C_{44} are, respectively, 4.349, 7.374 and 2.546.

From Table 1, it is clearly seen that the coefficient A is close to unity for the alloys, which allows us to say that these alloys are isotropic. The data in Table 1 indicate that the B/G ratio is between 2.3932 and 2.3730, that is the B/G ratio for materials is generally above the critical value of 1.75, which separates the ductile/brittle behaviors (brittle $< 1.75 <$ ductile) [17]

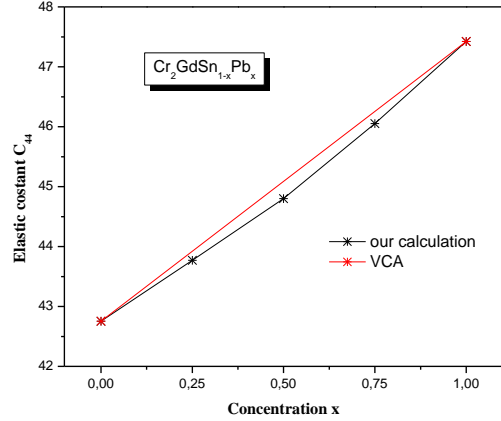
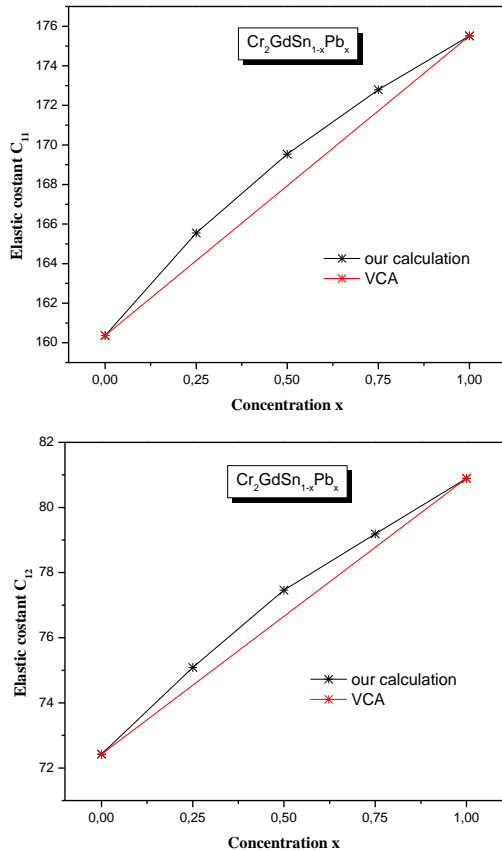


Fig. 4 – Variation of the elastic constants of $\text{Cr}_2\text{GdSn}_{1-x}\text{Pb}_x$

and allows us to classify the compounds as ductile materials. We know that the material becomes more solid the higher the E value; from Table 1, the Young's modulus decreases when we move from 0 to 1. We can say that Cr_2GdSn is stiffer than Cr_2GdPb . Our obtained values for Poisson's ratio vary from 0.3125 to 0.3152.

3.3 Electronic and Magnetic Properties

3.3.1 Band Structure

A good knowledge of the electronic band structure in materials provides valuable information concerning their potential utility in producing multi-electronic devices. We calculated the electronic band structure properties of Cr_2GdSn and Cr_2GdPb alloys using the GGA formalism. The calculated band structures of Cr_2GdSn and Cr_2GdPb alloys are illustrated in Fig. 5 and Fig. 6. First, for majority spins we notice an overlap of the valence and conduction bands, while the existence of electronic states at the Fermi level tells us about the metallic character of these alloys. As for minority spins, we note that the compounds studied have a semiconductor behavior with a band gap for compounds, that indicates that the compounds have a half-metallic behavior.

3.3.2 Total and Partial Densities of States

To take a deeper look at the electronic structure, we displayed in Fig. 7 the total and partial atomic site-decomposed density of states for Cr_2GdSn and Cr_2GdPb alloys. The occupied part of the valence bands can be subdivided into three regions. The first region is located from -11 eV to -8 eV below the Fermi level. This region is made up entirely of states 's' of Sn and Pb. The bands formed with states 'f' of Gd and 'd' of Cr are located around -5 eV to 0 eV. The third region is from 2 eV to 8 eV, the valence bands are dominated by states 'f' of Gd and orbital 'd' of Cr.

Densities of states confirm the metallic character for the majority of densities presented. At the minority-spin states, it is seen that there is a lack of electronic states at the Fermi level, which reveals the semiconductor character. This means that our compounds exhibit a half-metallic character in the two spin states. The values of the gap energy are listed in Table 2. It is noted that the values of the gap energy increase with the concentration of Pb.

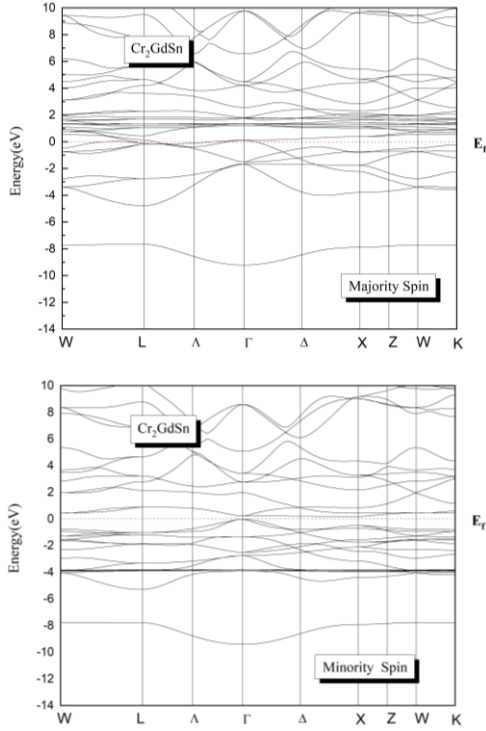


Fig. 5 – Calculated band structures of Cr_2GdSn Heusler alloy

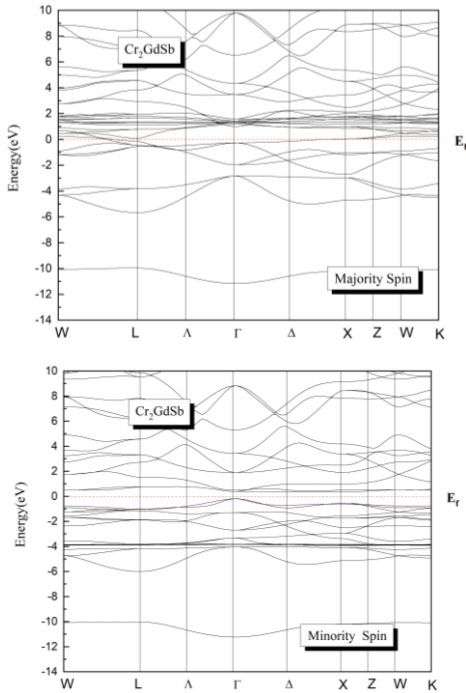


Fig. 6 – Calculated band structures of Cr_2GdPb Heusler alloy

3.3.3 Magnetic Behavior

The energy band structure of a half-metallic material has an asymmetry between the spin up and spin down states with an energy gap or a pseudo gap at the Fermi level. This gives rise to polarization of the conduction electrons at the Fermi level which can reach 100%. The obtained atomic and total magnetic moments of alloys $\text{Cr}_2\text{GdSn}_{1-x}\text{Pb}_x$ within GGA scheme along with other theoretical calculation values are reported in Table 3.

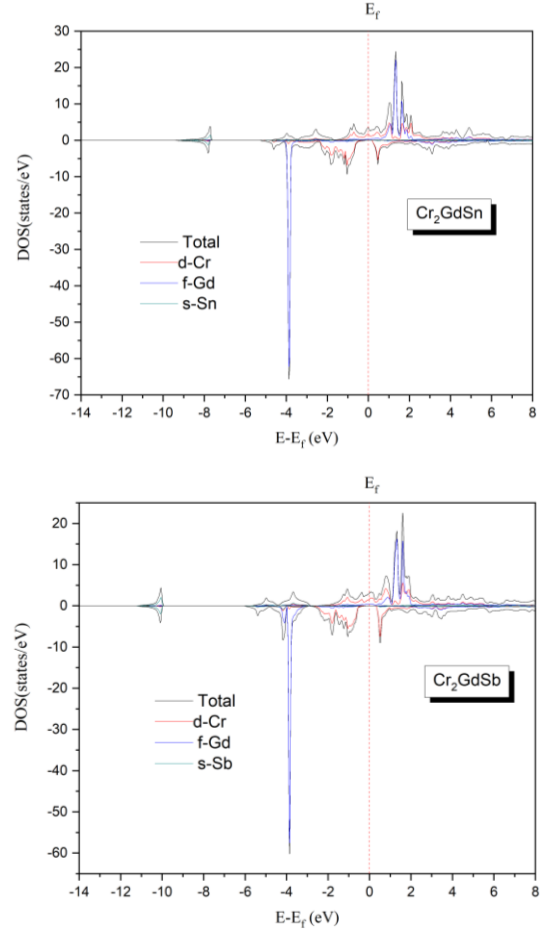


Fig. 7 – Total and partial density of states of Cr_2GdSn and Cr_2GdPb

We note that the main contribution in the magnetic moment is due to Gd and Cr atoms. The present test compounds Cr_2GdSn and Cr_2GdPb have a total magnetic moment of $-12.00\mu_B$ and $-11.00\mu_B$, respectively. Also note that the polarization values are 100% important which is characteristic of a half-metal. It is important to emphasize that we did not find any experimental or theoretical values of the magnetic moments for $\text{Cr}_2\text{GdSn}_{0.75}\text{Pb}_{0.25}$, $\text{Cr}_2\text{GdSn}_{0.50}\text{Pb}_{0.50}$, $\text{Cr}_2\text{GdSn}_{0.25}\text{Pb}_{0.75}$ and Cr_2GdSb .

3.4 Thermal Properties

One of the aims of this work is to study the thermodynamics of Heusler alloys. This study is of great importance in order to know their specific behavior when exposed to high pressures or temperatures.

Thanks to the quasi-harmonic Debye model implemented in the Gibbs program [17], we could study the thermal properties of $\text{Cr}_2\text{GdSn}_{1-x}\text{Pb}_x$ quaternary alloys. Through it, we could calculate the thermodynamic quantities of all the temperatures and pressures of the Heusler quaternary alloys from the $E-V$ data calculated at temperature = 0 and pressure = 0. In this part, we calculated the thermal properties in the temperature range from 0 to 1200 K under the influence of pressure in the range 0-20 GPa. The effect of temperature on the lattice parameters of $\text{Cr}_2\text{GdSn}_{1-x}\text{Pb}_x$ quaternary Heusler

Table 1 – Calculated lattice constant (a), bulk modulus (B), pressure derivative of the bulk modulus (B'), elastic constants (C_{ij}), shear modulus (G), B/G ratio, Young's modulus (E), Poisson's ratio (ν), Zener anisotropy factor (A), density (ρ) of $\text{Cr}_2\text{GdSn}_{1-x}\text{Pb}_x$ for various compositions

	Cr_2GdSn	$\text{Cr}_2\text{GdSn}_{0.75}\text{Pb}_{0.25}$	$\text{Cr}_2\text{GdSn}_{0.50}\text{Pb}_{0.50}$	$\text{Cr}_2\text{GdSn}_{0.25}\text{Pb}_{0.75}$	Cr_2GdPb
a (Å)	6.6902 6.6875 ^a	6.6596	6.6364	6.6183	6.5997
B (GPa)	100.8124 101.7384 ^a	105.2413	108.1526	110.3905	112.4328
B'	4.2148 4.3854 ^a	4.7194	3.5492	3.5566	4.4447
C_{11} (GPa)	159.2478 160.371 ^a	165.5529	169.5369	172.7949	175.5143
C_{12} (GPa)	71.2510 ^a 72.4220	75.0854	77.4604	79.1882	80.8917
C_{44} (GPa)	42.0142 42.7547 ^a	43.7710	44.8010	46.0526	47.4228
G (GPa)	42.1241 43.4226 ^a	44.5381	45.2959	46.3529	47.3783
B/G	2.3932 2.3429 ^a	2.3629	2.3876	2.3815	2.3730
E (GPa)	112.9842 113.6291 ^a	117.0961	119.2411	121.9850	124.6290
ν	0.3125 0.3138 ^a	0.3145	0.3162	0.3156	0.3152
A	0.9814 0.9722 ^a	0.9743	0.9731	0.9887	1.0023
ρ (g/cm ³)	5.1240 5.0815 ^a	5.1560	5.2206	5.2741	5.3295

^a Ref. [8]**Table 2** – Calculation of the band gap of $\text{Cr}_2\text{GdSn}_{1-x}\text{Pb}_x$ with Pb concentration x

Compound	x	E_g (eV)
$\text{Cr}_2\text{GdSn}_{1-x}\text{Pb}_x$	0.00	0.2103 0.2180 ^a
	0.25	0.2895
	0.50	0.3702
	0.75	0.4501
	1.00	0.5376

^a Ref. [8]**Table 3** – The total and partial magnetic moments (in μ_B) of $\text{Cr}_2\text{GdSn}_{1-x}\text{Pb}_x$

$\text{Cr}_2\text{GdSn}_{1-x}\text{Pb}_x$	m^{Cr}	m^{Gd}	m^{Sn}	m^{Sb}	m^{tot}	P (%)
Cr_2GdSn	- 2.1472 - 2.1363 ^a	- 6.9142 - 6.9712 ^a	0.0825 0.0904 ^a	- -	- 12.0074 - 12.0003 ^a	100 100 ^a
$\text{Cr}_2\text{GdSn}_{0.75}\text{Pb}_{0.25}$	- 2.0316	- 6.9672	0.0543	0.0630	- 11.7513	100
$\text{Cr}_2\text{GdSn}_{0.50}\text{Pb}_{0.50}$	- 2.0236	- 6.9024	0.0769	0.0886	- 11.4998	100
$\text{Cr}_2\text{GdSn}_{0.25}\text{Pb}_{0.75}$	- 1.9221	- 6.8852	0.0746	0.0866	- 11.2511	100
Cr_2GdSb	- 1.8681	- 6.8784	-	0.0732	- 11.0022	100

^a Ref. [8]

alloys with Sn concentration of 0, 0.25, 0.5, 0.75 and 1 is shown in Fig. 8. As expected, the volume increases with increasing temperature, and the rate of increase is high.

In Fig. 9, we report the evolution of the bulk modulus as a function of the temperature at different concentrations. According to this figure, we notice that the bulk modulus decreases with temperature. Heat capacity is one of the most important thermodynamic quantities because it provides information on vibration characteristics.

The heat capacity at constant volume C_V tends to the Petit Dulong limit at high temperatures [18]. C_V is pro-

portional to T^3 at sufficiently low temperatures. The temperature dependence of C_V is governed by the vibrations of atoms and for a long period can only be determined from experiments, and this is at medium temperatures [19]. Our results for $\text{Cr}_2\text{GdSn}_{1-x}\text{Pb}_x$ quaternary Heusler alloys concerning the heat capacity C_V at different temperatures are depicted in Fig. 10. There is a strong increase in C_V equal to 600 k. At higher temperatures and higher pressures, C_V tends towards the Dulong-Petit limit. The obtained values of the Dulong-Petit limit are $C_V(T) \cong 74.60 \text{ J}\cdot\text{mol}^{-1}\cdot\text{K}^{-1}$ for $\text{Cr}_2\text{GdSn}_{1-x}\text{Pb}_x$.

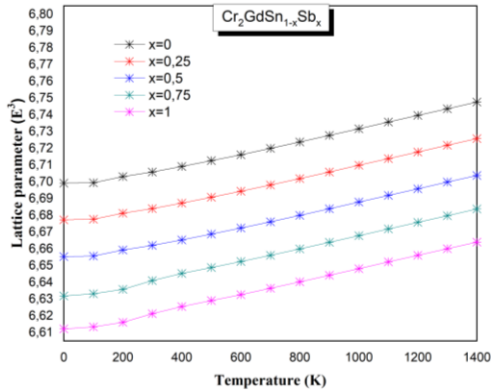


Fig. 8 – The lattice parameters of $\text{Cr}_2\text{GdSn}_{1-x}\text{Pb}_x$ as a function of temperature and Pb composition x

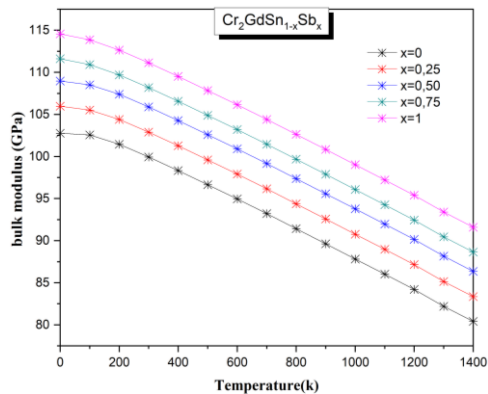


Fig. 9 – Variation of the bulk modulus as a function of temperature and Pb concentration x in $\text{Cr}_2\text{GdSn}_{1-x}\text{Pb}_x$ alloys

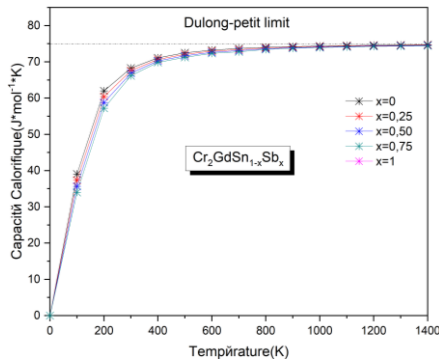


Fig. 10 – Variation of the heat capacity as a function of temperature and Pb concentration x in $\text{Cr}_2\text{GdSn}_{1-x}\text{Pb}_x$ alloys

In Fig. 11, we present the variation of the Debye temperature θ_D as a function of temperature and pressure, respectively, for the concentrations used. One can

observe that θ_D is nearly constant from 0 to 100 K and decreases linearly with increasing temperature from $T > 200$ K. The Debye temperature θ_D decreases linearly with increasing temperature, an increase in the concentration x leads to a Debye temperature increase as well as a bulk modulus increase.

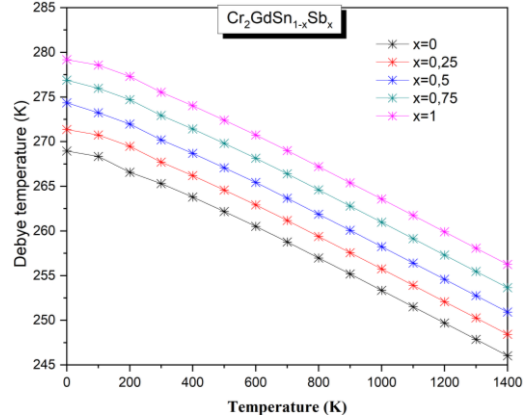


Fig. 11 – The Debye temperature θ_D as a function of concentration x for $\text{Cr}_2\text{GdSn}_{1-x}\text{Pb}_x$ alloy at various temperatures and pressures

4. CONCLUSIONS

Using the FP-LAPW method as implemented in WIEN2k code within GGA framework based on the DFT, we determined the structural, electronic, elastic and magnetic properties of $\text{Cr}_2\text{GdSn}_{1-x}\text{Pb}_x$ quaternary Heusler alloys. The results indicate that the AlCu_2Mn -type structure is energetically more stable than the CuHg_2Mn -type. The ground-state properties including the lattice parameter, bulk modulus, and its pressure derivatives were calculated. The estimated elastic constants confirm the mechanical stability of our compounds. The mechanical properties show that both compounds are anisotropic and ductile. Analysis of the density of states indicates a metallic behavior for $\text{Cr}_2\text{GdSn}_{1-x}\text{Pb}_x$, and the magnetic moment originates mainly from Gd and Cr atoms. The computed total magnetic moments are in very good agreement with Slater-Pauling rule and other recent theoretical investigations. We also successfully predicted thermodynamic properties, including heat capacity, thermal expansion and Debye temperature in different ranges of pressure and temperature using the quasi-harmonic Debye model. Finally, in the absence of experimental and theoretical works, the present results for the alloys studied provide an estimate of these materials which can be useful for further studies.

REFERENCES

1. R.A. de Groot, F.M. Mueller, P.G. van Engen, K.H.J. Buschow, *Phys. Rev. Lett* **50**, 2024 (1983).
2. F. Heusler, *Verhandlungen Dtsch. Phys. Ges* **5**, 219 (1903).
3. J. Winterlik, G.H. Fecher, C. Felser, *Solid State Commun.* **145**, 475 (2008).
4. T. Graf, C. Felser, S.S.P. Parkin, *Prog. Solid State Chem.* **39**, 1 (2011).
5. M. Parsons, J. Grandle, B. Dennis, K. Neumann, K. Ziebeck, *J. Magn. Magn. Mater.* **185**, 140 (1995).
6. K.H.J. Buschow, E.P. Wohlfarth, *Ferromagnetic Materials, Vol. 4* (Elsevier: Amsterdam: 1998).
7. H.C. Kandpal, G.H. Fecher, C. Felser, *J. Phys. D: Appl. Phys.* **40**, 1507 (2007).
8. I. Asfour, H. Rached, D. Rached, M. Caid, M. Labair, *J. Alloy. Compd.* **742**, 736 (2018).
9. W. Kohn, L.J. Sham, *Phys. Rev.* **140**, A1133 (1965).
10. P. Blaha, K. Schwarz, G.K. Madsen, D. Kvasnicka, J. Luitz, in *WIEN2k, An Augmented Plane Wave + Local Orbitals*

- Program for Calculating Crystal Properties* (Ed. by K. Schwarz) (Tech. Univ. Wien: Wien: 2001).
11. M.A. Blanco, A.M. Pendás, E. Francisco, J.M. Recio, R. Franco, *J. Mol. Struct. Theochem.* **368**, 245 (1996).
 12. I. Asfour, *Pramana – J. Phys.* **94**, 161 (2020).
 13. F. Murnaghan, *Proc. Natl. Acad. Sci. USA* **30**, 244 (1944).
 14. L. Vegard, *Z. Phys.* **5**, 17 (1921).
 15. I. Asfour, *J. Supercond. Nov. Magn.* **33**, 2837 (2020).
 16. W. Voigt, *Lehrbuch der Kristallphysik* (Teubner: Leipzig: 1928).
 17. M.A. Blanco, E. Francisco, V. Luana, *Comput. Phys. Commun.* **158**, 57 (2004).
 18. A.T. Petit, P.L. Dulong, *Ann. Chim. Phys.* 10395 (1819).
 19. P. Debye, *Ann. Phys.* **397**, 89 (1912).

Теоретичне моделювання структурної стабільності, еластичних, електронних, магнітних та термодинамічних властивостей нових напівметалевих сплавів $\text{Cr}_2\text{GdSn}_{1-x}\text{Pb}_x$

I. Asfour

Département de Technologie des Matériaux, Faculté de Physique, Université des Sciences et de la Technologie d'Oran Mohamed Boudiaf (USTO-MB), BP 1505, El M'naouer, 31000 Oran, Alegria

На основі методу повнопотенціальної лінеаризованої розширеної плоскої хвилі (FP-LAPW) у рамках теорії функціоналу щільності (DFT) досліджено структурні, пружні, електронні, магнітні, термодинамічні та теплові властивості четвертинних сплавів Гейслера $\text{Cr}_2\text{GdSn}_{1-x}\text{Pb}_x$ з використанням узагальненого градієнтного наближення (GGA). Структурні властивості показують стабільність сплавів $\text{Cr}_2\text{GdSn}_{1-x}\text{Pb}_x$ у феромагнітній фазі, де оцінюються їх рівноважні структурні параметри (стала решітки $a(\text{Å})$, об'ємний модуль B (ГПа) та його перша похідна від тиску (B')). Константи пружності для кубічної системи (C_{11} , C_{12} і C_{44}) та анізотропії розраховано для доказу механічної стабільності цих сполук. Результати дослідження електронних властивостей показують, що обидва сплави $\text{Cr}_2\text{GdSn}_{1-x}\text{Pb}_x$ мають ідеальну напівметалічну природу. Показано, що загальний магнітний момент кубічних сполук Cr_2GdSn та Cr_2GdPb дорівнює відповідно $-12\mu_B$ і $-11\mu_B$, що підтверджує їх повну напівметалеву поведінку. Квазігармонічна модель Дебая була реалізована в коді Гіббса та використовувалася для прогнозу теплових властивостей сплавів $\text{Cr}_2\text{GdSn}_{1-x}\text{Pb}_x$ як перспективних матеріалів для пристроїв спінтроніки.

Ключові слова: FP-LAPW, Електронні властивості, Феромагнітний, Напівметалічний, Модель Дебая.